Journal of Catalysis **192,** 316–321 (2000)
doi:10.1006/jcat.2000.2853, available online at http://www.idealibrary.com on IDEAL®

CO-Free Production of Hydrogen via Stepwise Steam Reforming of Methane

T. V. Choudhary and D. W. Goodman[1]

Department of Chemistry, Texas A&M University, P.O. Box 30012, College Station, Texas 77842-3012

Received October 13, 1999; revised February 15, 2000; accepted February 21, 2000

CO-free hydrogen is produced by the reversible cyclic stepwise steam reforming of methane for use in fuel cells and other processes that are sensitive to CO poisoning. The process consists of two steps involving the decomposition of methane in a first step followed by steam gasification of the surface carbon in a second step. The ease of carbon removal in step II is strongly dependent on temperature and surface coverage of carbon. To optimize the process conditions, we have investigated this cyclic methane steam-reforming process as a function of temperature and surface coverage of carbon. These studies show that it becomes increasingly difficult to remove the surface carbon at higher temperatures and coverage. Since higher temperatures favor methane conversion and hydrogen production in step I, it is essential to delicately optimize the temperature conditions for the process. The hydrogen produced in step I of the cyclic process in the optimum range of temperature conditions (≤673 K) is CO-free (<20 ppm). The amount of H_2 produced in step I varies from 1.0 to 1.3 mol/mol methane consumed. The optimum process conditions for carrying out the two-step process are temperatures of 648–673 K and a carbon surface coverage of 0.10–0.20 monolayer equivalents (MLEs).

1. INTRODUCTION

Fuel cell technology has seen a rapid development in the past decade, driven primarily by the fact that fuel cells are environmentally benign and have high efficiency. Processes such as steam reforming of methane, partial oxidation of methane, and autothermal reforming are the conventional sources of hydrogen (1–3). In practice, the level of residual CO (in the hydrogen stream) is unacceptable for the current proton-exchange membrane (PEM) fuel cells. The stringent requirement of <20 ppm CO in the hydrogen stream adds substantial cost to the operation of fuel cells using hydrogen from these conventional sources. Hence, there are obvious economic incentives for the production of CO-free hydrogen from methane.

Decomposition of methane has been studied quite extensively for methane homologation reactions (4, 5) and fundamental dynamical studies (6); however, methane decomposition as a method to obtain hydrogen has received relatively little attention (7, 8). It has been shown that, at temperatures greater than 823 K, Ni-based catalysts exhibit stable operation for a few hours, providing 2 mol of H_2/mol of methane reacted (8, 9). The absence of rapid catalytic deactivation is explained by the diffusion of carbonaceous residues into the bulk of the metal particles. The latter process generates active surface sites for dehydrogenation of subsequent methane molecules, resulting in the formation of filamentous carbon. But at these high temperatures carbon is expected to exist in the graphitic form, making it very difficult to remove a large fraction of the surface carbon by methods other than oxidation. Though the oxidation process is able to restore the initial activity of the catalyst, high-temperature oxidation results in sintering of the metal particles. Another disadvantage of the use of high temperatures for decomposition of methane is the possible formation of CO via reaction of the carbonaceous residue with oxygen of the oxidic support (11).

Based on preliminary work, we have recently proposed stepwise steam reforming of methane to produce CO-free hydrogen (12). This process, which operates at relatively low temperatures, involves the catalytic decomposition of methane in a first step to produce CO-free hydrogen and surface carbon and/or hydrocarbonaceous species (step I),

$$CH_4 \rightarrow C_{ads}/[C(H)_n]_{ads} + (2 - n/2)H_2,$$

followed by a separate step in which the carbon and/or hydrocarbonaceous species is removed via reaction with water (step II), regenerating the catalyst with respect to step I:

$$C_{ads}/[C(H)_n]_{ads} + H_2O \rightarrow CO_2 + (2 + n/2)H_2.$$

In our preliminary experiments (12) hydrogen was passed over the catalyst between cycles (cycle = step I + step II). In the present study no hydrogen was passed between cycles. Previously, reaction cycles were reported on a Ni/zirconia catalyst at 648 K at a single coverage of carbon. These studies have been extended since it is very important to investigate the effect of temperature and carbon coverage

[1] To whom correspondence should be addressed. E-mail: goodman@mail.chem.tamu.edu. Fax: (409) 845-6822.

0021-9517/00 $35.00

on the overall process to optimize conditions for this process. The temperature effect is critical since it is known that carbon (on the Ni catalyst surface) changes from a carbidic/amorphous (reactive) form to a graphitic (unreactive) form at ~650 K (13). This transition is also enhanced with an increase in the surface carbon coverage.

In this work we have used GC pulse experiments to study the stepwise steam reforming of methane as a function of temperature and carbon coverage. CO pulse experiments have been carried out to measure the specific metal surface area; TEM has been used to find the particle size and the nature of the surface carbon.

2. EXPERIMENTAL

a. Catalyst Synthesis

Ni supported on zirconia was selected for this process, based on the work of Moore and Lunsford, which dealt with step II of the reaction (14). The Ni/zirconia (88% Ni by weight) catalyst was prepared by coprecipitation of the hydroxides from a basic solution of the nitrate salts. The resulting gel was filtered, washed with distilled water, and then dried at 338 K overnight. Following this, the catalyst was oxidized in air for 2 h at 473 K and at 673 K for 2 h. The powder catalyst was then pressed, crushed, and sieved to a size of 20–40 mesh. Before the reaction, the catalyst was reduced with H_2 in flowing He at a total flow rate of 20 ml/min for 30 min at 523 K and at 723 K for 15–16 h. Following this, the catalyst was flushed with the carrier gas for 1 h and heated to the desired temperature in a flow of the carrier gas.

b. Apparatus and Analytical Techniques Used for the Study

A pulse reactor unit consisting of a stainless steel (SS) reactor, a furnace controlled by a temperature controller, a cold trap for trapping water, and gas chromatographs (GCs) (TCD + FID) was used in these studies. The SS reactor was 10-in. long with $\frac{1}{4}$-in. o.d. with a small section serving as the catalyst bed. A ceramic rod and glass beads were placed on either side of the catalyst bed to secure its position. In the first step, a (5% CH_4 in He/Ar) pulse of 1.65 ml was introduced into the catalyst via a He/Ar carrier gas. Following this, a 1- to 2-μl pulse of water was introduced into the heated zone of the catalyst reactor. Analysis of the gases was carried out via an on-line GC with TCD using He as the carrier gas. Separate experiments were carried out using argon as the carrier gas for detection of hydrogen (all other conditions remaining the same). A (10 ft × $\frac{1}{8}$ in.) Hayasep DB column at room temperature was used for separation of the gases. Unreacted water was trapped prior to the Hayasep DB column by a trap cooled with a slurry of acetone and dry ice. Occasionally, the products from the TCD were routed to a FID (via a methanizer) for detection of CO during step I of the process. With this arrangement, very small amounts of CO (>15 ppm in the product stream) could be measured.

c. Catalyst Characterization

Specific surface area measurement. The Ni surface area was measured by CO pulse adsorption experiments carried out at room temperature, assuming a CO/Ni ratio of 1.0. Prior to the Ni surface area determination, the catalyst was prereduced at 723 K for a period of 15 h in flowing H_2 and He and then brought to room temperature in flowing He; analysis of CO was carried out on-line with a TCD. The exposed Ni surface area was determined to be 5.8 ± 0.3 m^2/g.

TEM characterization. TEM micrographs of the zirconia-supported Ni catalyst were obtained using a high-resolution Jeol 2010 instrument (Electron Microscopy Center: Texas A&M University). Samples used in the chemisorption measurements and after reaction were ultrasonically dispersed in acetone and spread over perforated molybdenum grids. Several bright field TEM micrographs of different portions of the sample were obtained at magnifications up to 400,000. From the TEM micrographs the particle size for the zirconia-supported Ni catalyst was found to lie in the range of 70–110 nm.

Catalyst deactivation. The catalyst was first pretreated as mentioned earlier. Following this, pulses of 5% CH_4 in He were passed over the catalyst sequentially. Figures 1a and 1b show the deactivation profiles for two different catalyst loadings (100 and 200 mg) at 648 K. From the figures, rapid deactivation is observed initially followed by a period of slow deactivation. Finally, the activity stabilizes at a steady-state value. No filamental carbon formation was observed via TEM in the above experiments.

3. RESULTS AND DISCUSSION

Each cycle of the reaction sequence consists of two steps: methane decomposition resulting in the production of hydrogen and a hydrocarbonaceous species on the surface followed by steam gasification of the surface carbon. Figure 2a shows 20 reaction cycles at 648 K on a 100 mg of Ni/zirconia catalyst. The amount of methane reacted (step I) is denoted by data points below the abscissa, whereas the gas phase carbon-containing products (CH_4 and CO_2) obtained in step II are shown above the abscissa. The average methane conversion obtained in each pulse (1.65 ml of 5% CH_4 in He) was ~75% at a total GHSV of 18,000 $cm^3\ g^{-1}\ h^{-1}$. It is apparent that there is no detectable loss of catalytic activity throughout the 20 cycles. The amount of surface carbon removed in step II varied from 85% to 95% (of the amount deposited in step I) in the various cycles. The average amount of surface carbon

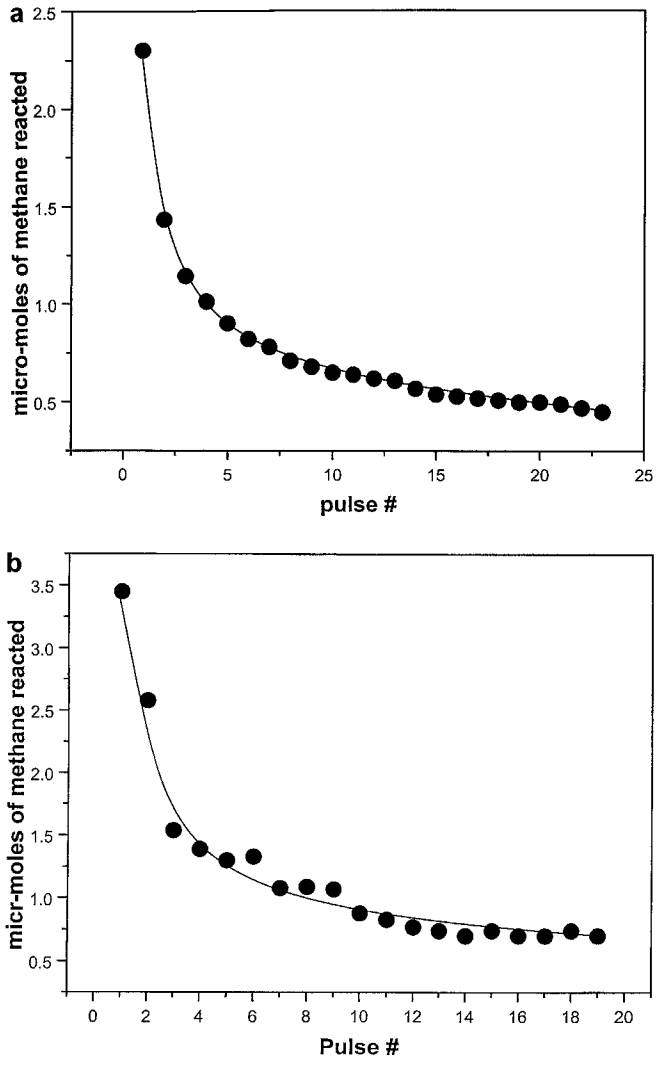

FIG. 1. Deactivation profiles for two catalyst (Ni/zirconia) loadings: (a) 100 mg and (b) 200 mg.

removed in step II was 88%. The unreacted carbon remaining after the second step is believed to be stored on the support via metal-to-support carbon migration as suggested in previous studies (15, 16). In all reaction cycles the percentage of carbon removed in the first cycle was observed to be more than that for subsequent cycles. These results are likely due to the fact that the initial reaction takes place on a freshly hydrogenated catalyst surface. Also, the initial activity of the catalyst for methane decomposition was slightly lower for the first cycle and then it stabilized to a fixed value for the later cycles. Only hydrogen was obtained as a product in step I, the concentration of CO being <20 ppm. The main products observed in step II were hydrogen, CO_2, and CH_4; the amount of CO obtained was <0.2%. The average selectivity for methane obtained in step II was 23%. The selectivity for methane in step II of the first cycle was considerably larger than that of subsequent cycles. The average molar amount of H_2 produced per mole of methane consumed in step I was 1.1 and the total molar amount of H_2 produced per mole of methane consumed including step I and step II was 3.0. Figure 2b shows the same data in the form of carbon buildup on the surface as a function of the number of reaction cycles. The parallel behavior of the two sets of data shows that there was no decrease in activity of the catalyst between each cycle. Figure 3 shows 15 reaction cycles at 673 K on a 100 mg of Ni/zirconia catalyst. There was no drop in activity of the catalyst throughout the 15 cycles, and on average, 86% of the carbon was removed in step II. The average selectivity for methane obtained in step II was 22%; the CO in the step I hydrogen was <20 ppm. In these experiments 1.2 mol of H_2/mol of methane consumed was produced in step I. Figure 4 shows 15 reaction cycles at 673 K on 50 mg of catalyst; the selectivity for methane in step II was 22%. Although the average amount of carbon removed in step II was only 75%, no decrease in activity of the catalyst was observed. There is no

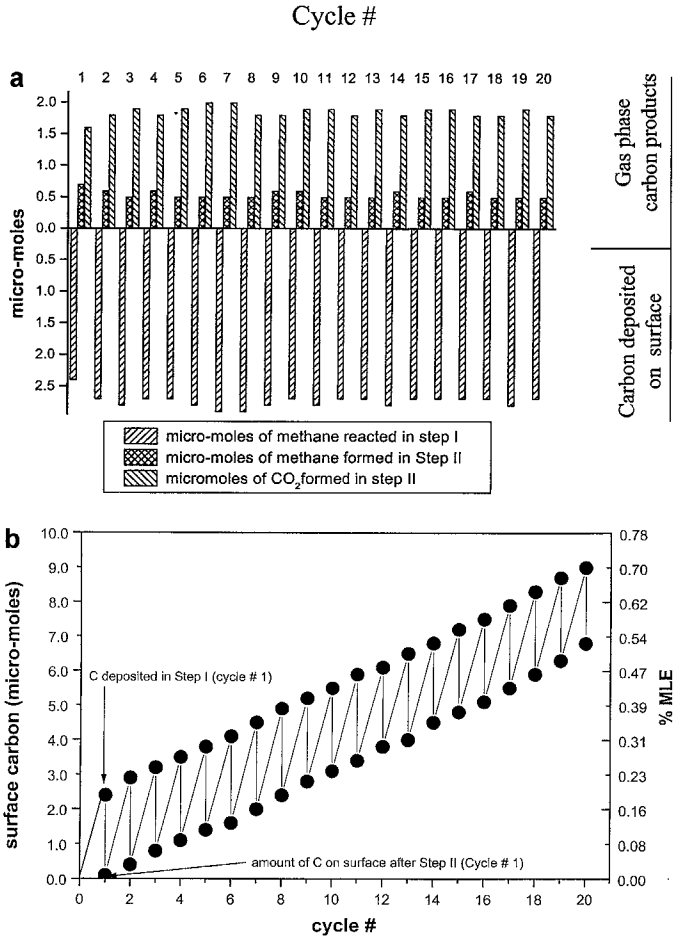

FIG. 2. Twenty reaction cycles at 648 K on a 100 mg of Ni/zirconia catalyst: (a) shows the data in the form of reactants and products as a function of cycle number and (b) shows the carbon buildup on the surface as a function of cycle number.

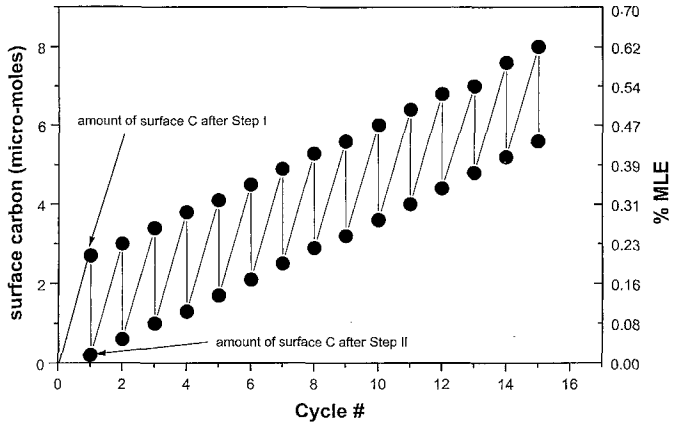

FIG. 3. Carbon buildup on the surface as a function of cycle number for 15 reaction cycles at 673 K on a 100 mg of Ni/zirconia catalyst.

apparent rollover in the activity near monolayer coverage in Fig. 4, indicating that the carbon growth on the surface is three-dimensional. Presumably then, many reaction cycles can be carried out prior to the necessity for oxidative regeneration of the catalyst.

Effect of Surface Coverage of Carbon

In these experiments the temperature was kept constant and the surface coverage of carbon was varied. This was achieved by using different catalyst loadings and maintaining the amount of methane (introduced to the catalyst) in step I constant. The effect of surface carbon coverage on step II of the reaction (removal of surface carbon) was studied at two different temperatures. The surface carbon (monolayer equivalents, MLE) was estimated from the specific metal surface area, assuming 1 monolayer to correspond to a $C/Ni_{surface}$ ratio of 1.0. Figures 5a and 5b show the average carbon removed in step II as a function of MLE of carbon deposited in step I of each cycle at 648 and 673 K, respectively. At 648 K, 93% (average of all cycles) of

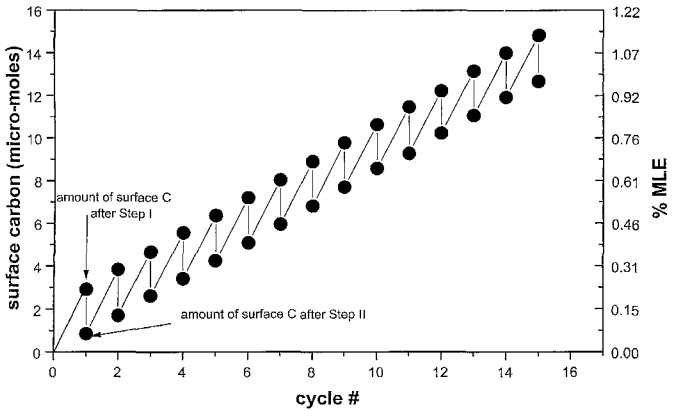

FIG. 4. Carbon buildup on the surface as a function of cycle number for 15 reaction cycles at 723 K on a 100 mg of Ni/zirconia catalyst.

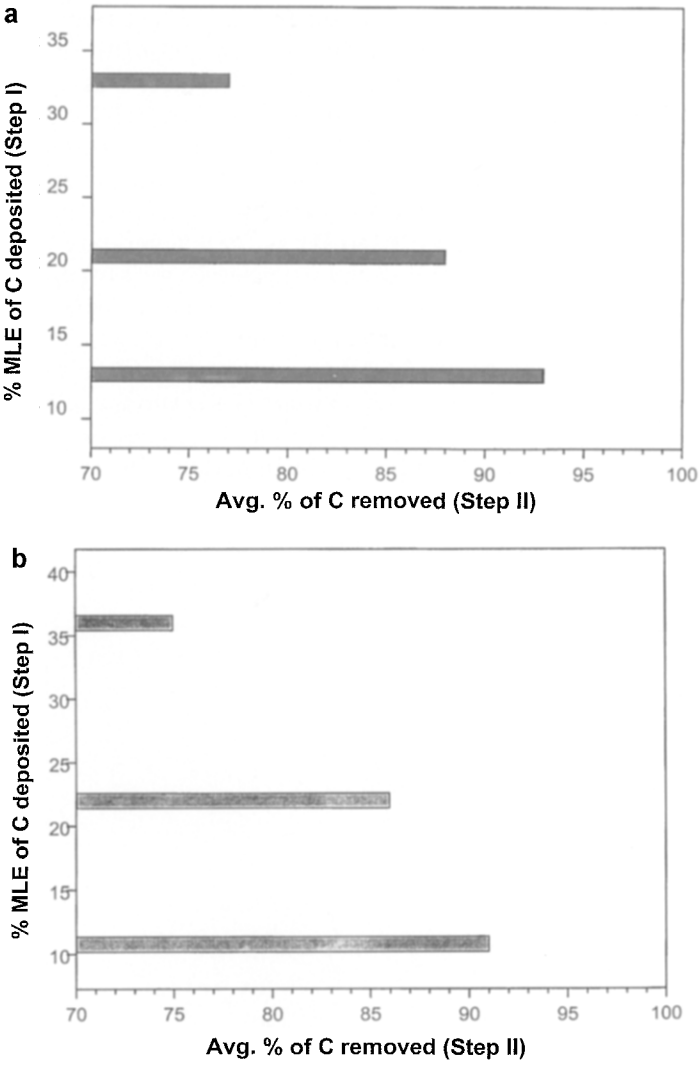

FIG. 5. Average percentage of carbon removed in step II as a function of percentage MLE deposited in step I of each cycle at (a) 648 K and (b) 673 K.

the surface carbon could be removed in step II upon deposition of 0.13 MLE carbon in step I (Fig. 5a). This decreased to 77% when the MLEs of carbon deposited on the surface was 0.33. A similar trend was observed at 673 K (Fig. 5b). There is a dramatic increase in the difficulty of removal of carbon in step II at higher carbon coverages, suggesting a transition from the more reactive amorphous/carbidic form to the less reactive graphitic form at the higher carbon coverages.

Effect of Temperature

To address the effect of temperature, the surface carbon coverage was kept constant and the temperature varied. Figure 6a shows the effect of temperature on step II; the surface carbon coverage in each case was 0.13 MLEs. The data of Fig. 6a indicate an increasing resistance to carbon

removal with an increase in temperature. The carbon removed in step II was essentially constant (93–91%) in the temperature range 623–673 K; however, there was a significant decrease in the carbon removed at 723 K (only 85% of the deposited carbon could be removed). This may be attributed to the change in form of the surface carbon (active → graphitic-like). Also, there was a decrease in the selectivity for methane (step II) as the temperature was increased (Fig. 6b). This decrease in selectivity is expected since it should be easier to form methane (rather than CO_2) from surface $-CH_2$ species than from–CH species (more likely to dominate at higher temperatures). Further work is in progress to confirm the nature of the surface hydrocarbonaceous species using high-resolution electron energy loss spectroscopy (HREELS). The importance of temperature in this study is apparent. Higher temperatures favor methane conversion and higher production of hydrogen

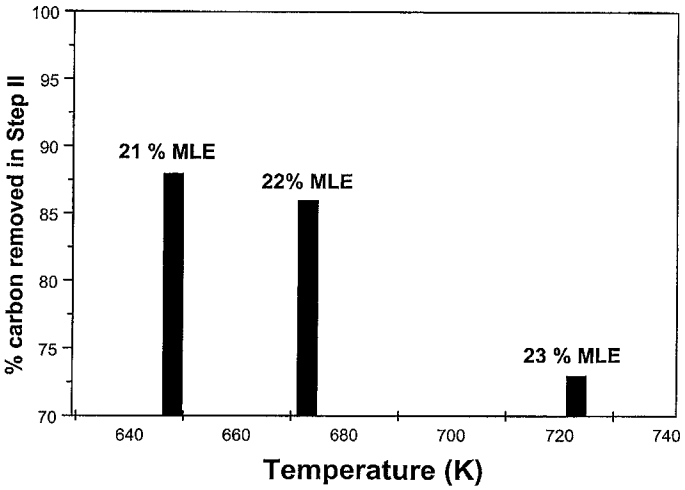

FIG. 7. Average percentage of carbon removed in step II as a function of temperature at a surface coverage greater than 20%.

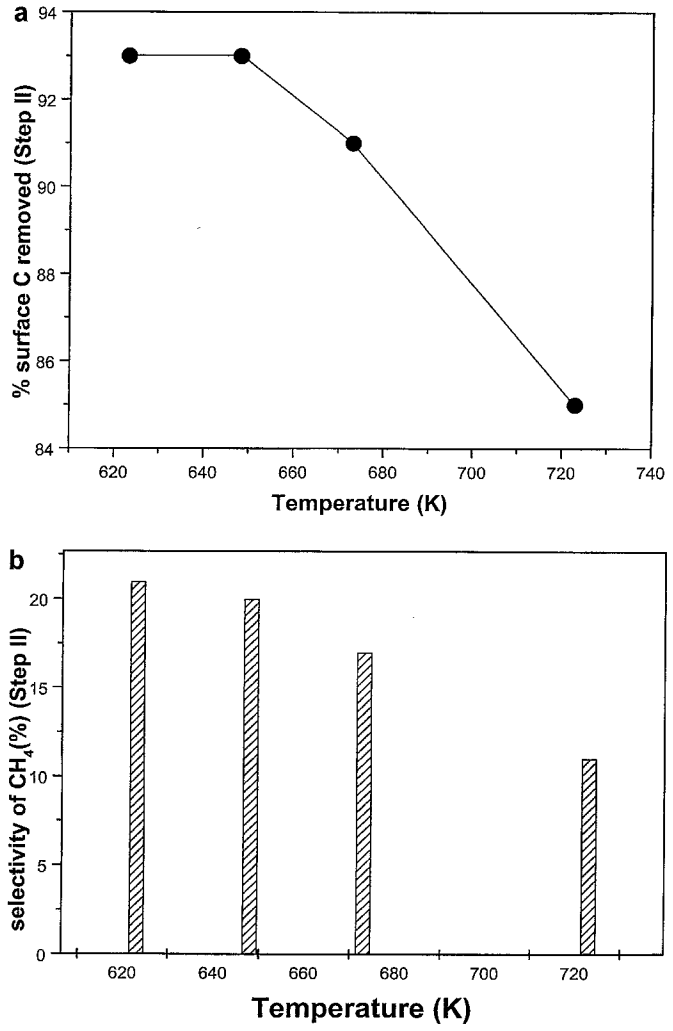

FIG. 6. (a) Average percentage of carbon removed and (b) selectivity for methane formed in step II as a function of temperature at a constant surface coverage of 13% MLE.

per mole of methane consumed. However, at temperatures >673 K, more than 20 ppm CO was observed in the gas stream (step I). This follows since higher temperatures thermodynamically favor CO formation. The CO formed in step I arises mainly via reaction of surface carbonaceous species with the oxygen of the oxidic support (11). CO may also be formed (step I) at higher temperatures by reaction with a slightly oxidized surface formed in step II (regeneration with steam). The amount of CO in the step I hydrogen was found to be <20 ppm for temperatures below 673 K. As shown earlier, higher temperatures inhibit carbon removal in step II, with the effect being more pronounced at the higher carbon coverages. Figure 7 shows the effect of temperature on step II at high carbon coverage (0.21–0.23 MLEs). A significant decrease in the carbon reactivity is apparent with increasing temperature. The amount of carbon removed in step II decreased from 88% at 648 K to 73% at 723 K, clearly indicating a larger resistance for carbon removal at higher temperature and higher surface coverage. These studies are in good agreement with methane homologation investigations where the percentage of active carbon (formed after the methane decomposition step) was found to decrease with increasing temperatures and surface coverage (17, 18). Working within the temperature range of 648–673 K and a carbon coverage of 0.10–0.20 MLEs, most of the surface carbon can be removed in step II to obtain CO-free hydrogen (<20 ppm) in step I of this two-step cyclic process.

4. CONCLUSIONS

Stepwise steam reforming of methane for production of CO-free hydrogen has been investigated at various process conditions. Numerous reaction cycles have shown the process to be feasible for the production of CO-free hydrogen. The data show that there is a delicate temperature range

within which the process can be successfully employed. Although high temperature favors step I of the process, it is detrimental to step II. An increase in the surface carbon coverage has a negative impact on the removal of surface carbon (step II). This effect of temperature and surface carbon coverage is explained by a transition of active to inactive surface carbon.

The overall process runs optimally between 648–673 K and a surface carbon coverage of 0.10–0.20 MLEs. Under these conditions the process can be operated in cycles to obtain CO-free hydrogen in step I (1.0–1.2 mol of H_2/mol of CH_4 consumed). The hydrogen produced in step II of this process contains <0.5% CO. The methane obtained in step II can be recycled (to step I) to enhance the overall yield of CO-free hydrogen.

ACKNOWLEDGMENTS

We acknowledge with pleasure the support of this work by the Department of Energy, Office of Basic Energy Sciences, Division of Chemical Sciences. T. V. Choudhary would like to thank T. P. St. Clair and Valerii Bukhtiyarov for their helpful suggestions during the course of this work.

REFERENCES

1. Rostrup-Nielson, J. R., *Catal. Today* **18**, 305 (1993).
2. Choudhary, V. R., Rajput, A. M., and Prabhakar, B., *Angew. Chem. Int. Ed. Engl.* **33**, 2104 (1994).
3. Armor, J. N., *Appl. Catal. A* **176**, 159 (1999).
4. Koerts, T., Deelan, M. J., and Van Santen, R. A., *J. Catal.* **138**, 101 (1992).
5. Koranne, M. M., and Goodman, D. W., *Catal. Lett.* **30**, 219 (1995).
6. Beebe, T. P., Jr., Goodman, D. W., and Yates, J. T., Jr., *J. Chem. Phys.* **87**, 2305 (1987). Wu, M.-C., and Goodman, D. W., *Catal. Lett.* **24**, 23 (1994). Lenz-Solomun, P., Wu, M.-C., and Goodman, D. W., *Catal. Lett.* **25**, 75 (1994). Wu, M.-C., and Goodman, D. W., *Surf. Sci. Lett.* **306**, L529 (1994). Wu, M.-C., Xu, Q., and Goodman, D. W., *J. Phys. Chem.* **98**, 5104 (1994).
7. Muradov, N. Z., *Energy Fuels* **12**, 41 (1998).
8. Zhang, T., and Amiridis, M. D., *Appl. Catal. A* **167**, 161 (1998).
9. Snoeck, J. N., Froment, G. F., and Fowles, M., *J. Catal.* **169**, 250 (1997).
10. Kuvshinov, G. G., Mogilnykh, Y. I., and Kuvshinov, D. G., *Catal. Today* **42**, 357 (1998).
11. Ferreira-Aparicio, P., Rodriguez-Ramos, I., and Guerrero-Ruiz, A., *Appl. Catal. A* **148**, 343 (1997).
12. Choudhary, T. V., and Goodman, D. W., *Catal. Lett.* **59**, 93 (1999).
13. Goodman, D. W., Kelley, R. D., Madey, T. E., and Yates, J. T., Jr., *J. Catal.* **64**, 479 (1980).
14. Moore, S. E., and Lunsford, J. H., *J. Catal.* **77**, 297 (1982).
15. Solymosi, F., Erdohelyi, A., Cserenyi, J., and Felvegi, A., *J. Catal.* **147**, 272 (1994).
16. Soltan Mohammad Zadeh, J., and Smith, K. J., *J. Catal.* **176**, 115 (1998).
17. Guczi, L., Van Santen, R. A., and Sarma, K. V., *Catal. Rev.–Sci. Eng.* **38**, 249 (1996), and references therein.
18. Soltan Mohammad Zadeh, J., and Smith, K. J., *J. Catal.* **183**, 232 (1999).